$BaMgAl_{10}O_{17}$ as host matrix for Mn in the catalytic combustion of methane

Marcel Astier, Edouard Garbowski*, and Michel Primet

Université Claude Bernard LYON I, L.A.C.E., 43 boulevard du 11 Novembre 1918, 69622 Villeurbanne Cedex

Received 16 December 2003; Accepted 2 March 2004

$BaMgAl_{10}O_{17}$ (BMA) solid has been prepared by a sol–gel process: after calcination at 1200 °C a regular structure is obtained along with BET area of 13 m^2 g^{-1}. Unexpectedly this solid is active in the catalytic combustion of methane, and its activity is comparable to the activity of other hexaaluminates containing transition metal ions. This activity may be due to oxygen ion diffusion through the mirror plane in relation with a charge compensation mechanism induced by the presence of Mg^{2+} ions. The introduction of Mn ions does not alter the structure but leads to the same phenomenon due to the presence of Mn^{2+} ions. A minor amount of Mn^{3+}, revealed by hydrogen TPR and by reflectance spectroscopy, is responsible for an enhanced oxidation activity and a lowering of the activation energy. Such BMA materials may have interesting properties as oxidation catalyst.

KEY WORDS: methane; catalytic combustion materials; hexaaluminate; sol–gel; manganese.

1. Introduction

Catalysts for high temperature combustion of methane need to be heat resistant when high power is required as for electricity generation with gas turbine [1]. Some new phases meeting such requirement appeared recently: they are based on barium cation-substituted hexaaluminate $BaM_xAl_{12-x}O_{19-\alpha}$ where M may be Cr, Mn, Fe, Co, Ni or Cu [2–6]. The high resistance to sintering is attributed to the β-alumina crystal structure [6–8], where crystals do have the shape of small plates. They consist of alumina spinel layers separated by layers containing bulkier alkali or alkaline earth cations, preventing any alumina fusion between layers. Barium magnesium aluminium oxide $BaMgAl_{10}O_{17}$ (BMA) which crystallises in the hexagonal system belongs to the same space group [9] as $BaAl_{12}O_{19}$ [10]. The refined crystal structure of BMA [11] agrees with that of $Ba_{0.75}Al_{11}O_{17.25}$ refined by Iyi *et al.* [12] as a defective β-alumina type. It may therefore present similar properties and possibilities of substitution of the Al^{3+} ions. These materials have been widely used as host matrix for Eu^{2+} giving blue emitting phosphor [13,14] and sometimes for both Eu^{2+} and Mn^{2+} giving green emitting phosphor [15] as well as solid electrolytes in chemical sensors [16]. So far their use in heterogeneous catalysis has been completely ignored and no work and no report seem to have been recorded up to now. The introduction of some active cations like Mn in barium hexaaluminate (BA) as substitute for Al leads to active and thermo stable catalysts for the combustion of methane [2]. Therefore a BMA host matrix and a manganese substituted one of theoretical composition $BaMgAl_9MnO_{17}$ (BMA–Mn) were prepared, characterised and tested in this reaction.

* To whom correspondence should be addressed.
E-mail: Edouard.Garbowski@univ-lyon1.fr

2. Preparation

The samples were prepared by a sol–gel method. An aqueous solution of barium acetate and magnesium acetate (0.05 mol of each in 200 cm^3 of water) was mixed under a vigorous stirring into an alcoholic solution of aluminium 2-butanolate $(C_4H_9O)_3Al$ (0.5 mol in 300 cm^3 of propan-2-ol). The alumina gel formed was allowed to stand overnight before drying in a rotating evaporator under reduced pressure. The elimination of the solvent was completed by heating for one night at 120 °C. For the preparation of the BMA–Mn sample 0.05 mol of manganese acetate is added to the aqueous solution and only 0.45 mol of aluminium 2-butanolate is used.

The two dried solids were treated in a similar way: heating up to 500 °C (3 h) and 1200 °C (12 h) using a heating rate of 4 °C/min^{-1} under a flow of pure oxygen to ensure complete organic precursors elimination by combustion and solid state reaction.

3. Characterisations and results

3.1. BET area

The BET surface areas were measured on a computerised laboratory made BET apparatus. The BET areas calculated from nitrogen adsorption at 77 K after out gassing for 2 h at 500 °C were 13 m^2 g^{-1} for BAM and

1011-372X/04/0500–0031/0 © 2004 Plenum Publishing Corporation

10 m^2 g^{-1} for BAM–Mn. These values are typical and similar to the Ba hexaaluminates previously reported [2,5,6].

3.2. X-ray diffraction analysis

The X-ray diffraction diagrams were recorded using a SIEMENS D500 diffractometer using the $K_{\alpha 1}$ line at 1.5406 Å. For both samples figure 1a and b show only lines which can be attributed to BMA [10] and $BaAl_2O_4$ [17] (pointed by arrows), no other crystalline phase seems to be present. The lattice parameters and the 'c/a' ratio in the hexagonal system were carefully calculated by a least square method using a spreadsheet. The values are given in table 1 and also compared to values of parameters found in the literature. The parameters for $BaAl_2O_4$ cannot and were not calculated because only three lines belonging to this compound are clearly evidenced on the XRD diagrams. These results are in total agreement with the observations of Smets and Verlijdonk [15] stating that the incorporation of Mn^{2+} results in the formation of a solid solution between $BaMgAl_{10}O_{19}$ and a low Ba content hexaaluminate having exactly the same structure. The 'a' parameter is higher for BMA–Mn. The difference is small but significant and higher than the experimental error. It is about the same as the difference observed for the substitution of 1 aluminium ion by 1 manganese ion in $BaAl_{12}O_{19}$ [2,18]. Moreover the most intense line which corresponds to the (107) plane for BMA (figure 1a) corresponds to the (114) plane for BMA-Mn (figure 1b). It is therefore possible to conclude to a true substitution of one aluminium ion by one Mn ion in the structure. The value of the 'c/a' ratio for BMA–Mn calculated in this study is comparable to the value given for BMA [14]. This suggests that Mn ions could also take the same kind of sites as the Mg ions sites.

3.3. Diffuse reflectance spectroscopy

The UV-visible diffuse reflectance spectra were recorded using a PE Lambda 9 spectrometer equipped with an integrating sphere at room temperature using $BaSO_4$ as reference. For BMA–Mn two main intense bands were located close to 300 and 500 nm, and a broad one of lower intensity located between 800 and 1200 nm are observed (figure 2a). This BMA–Mn is a strongly brown-yellow solid, whereas BMA is white and does not show any band and therefore the spectrum is not reported. Thus the observed bands are necessarily related to Mn^{x+} ions. The band at about 300 nm is relatively intense and should correspond to a charge transfer between oxygen anion and manganese cation (ligand to metal charge transfer, LMCT) because (i) no d–d transitions are possible at such energies for the first series of transition metal ions (ii) no d–d transition with such a low manganese concentration should have such high intensity.

Among the various possible oxidation states of Mn(+2, +3, +4), remembering that MnO_2 is not stable above 773 K [19,20], Mn^{4+} is very unlikely to be present in solids prepared at high temperature (1200 °C). On the other hand due to a high-spin d^5 electronic structure, Mn^{2+} leads to totally spin-forbidden bands and appears always almost transparent [21]. Therefore for the highly coloured solid, Mn^{3+} ion is the only one which could account for the band observed at 500 nm corresponding to the unique spin-allowed d–d transition for a d^4 electronic configuration. When such ion is located in an octahedral coordination, Jørgensen recorded an absorption maximum around 20,000 cm^{-1} or 500 nm [22]. If the absorbance is plotted as a function of the wave number (figure 2b), rather than wavelength as it is usual, this band is more clearly evidenced as well as the second one near 10,000 cm^{-1}. This second band was also reported close to the same wave number (or wavelength) by the same author, who concluded to a spin forbidden transition, for example in the case of the $Mn(OX)_3^{3-}$ complex (OX is oxalate). This plot also shows that the band attributed to a charge transfer between oxygen anions and manganese cations (LMCT) is very wide and must correspond to a combination of several bands, at least two. This observation together with the presence of a spin forbidden transition lead to the conclusion that Mn^{3+} ions are present in sites of octahedral symmetry, and that some of them are probably located in distorted octahedral ones.

3.4. Temperature programmed reduction

The temperature programmed reduction of the matrix and of the catalyst was performed with 1 vol% H_2 in He starting from room temperature up to 1273 K with a heating rate of 15 K min^{-1} and a flow rate of 20 cm^3 min^{-1}. Hydrogen consumption is monitored by mass spectrometry. The results in figure 3 show only a very small reduction peak with a maximum at 950 K for the BMA matrix. By contrast for the BMA–Mn catalyst a large peak with a maximum located at 700 K is observed together with another one above 900 K. A resolution into two reduction peaks may be performed easily. Assuming a Gaussian shape for the peaks observed for the Mn substituted catalyst the contribution of each one can be calculated. The maximum of the first peak is located at 700 K and the H_2 consumption is 163 μmol g^{-1} whereas the location of the second peak is 950 K and corresponds to 67 μmol g^{-1} giving a total amount of 230 μmol g^{-1} of H_2. The amount of Mn determined by chemical analysis is 1.6 10^{-3} mol g^{-1}. Assuming that Mn^{3+} is reduced to Mn^{2+}, only 28% of Mn is present as Mn^{3+} ions, 70% being reduced at 700 K (first peak) and 30% less reducible at 950 K. This observation of two peaks is in agreement with the hypothesis of at least two different octahedral sites for the location of Mn^{3+}.

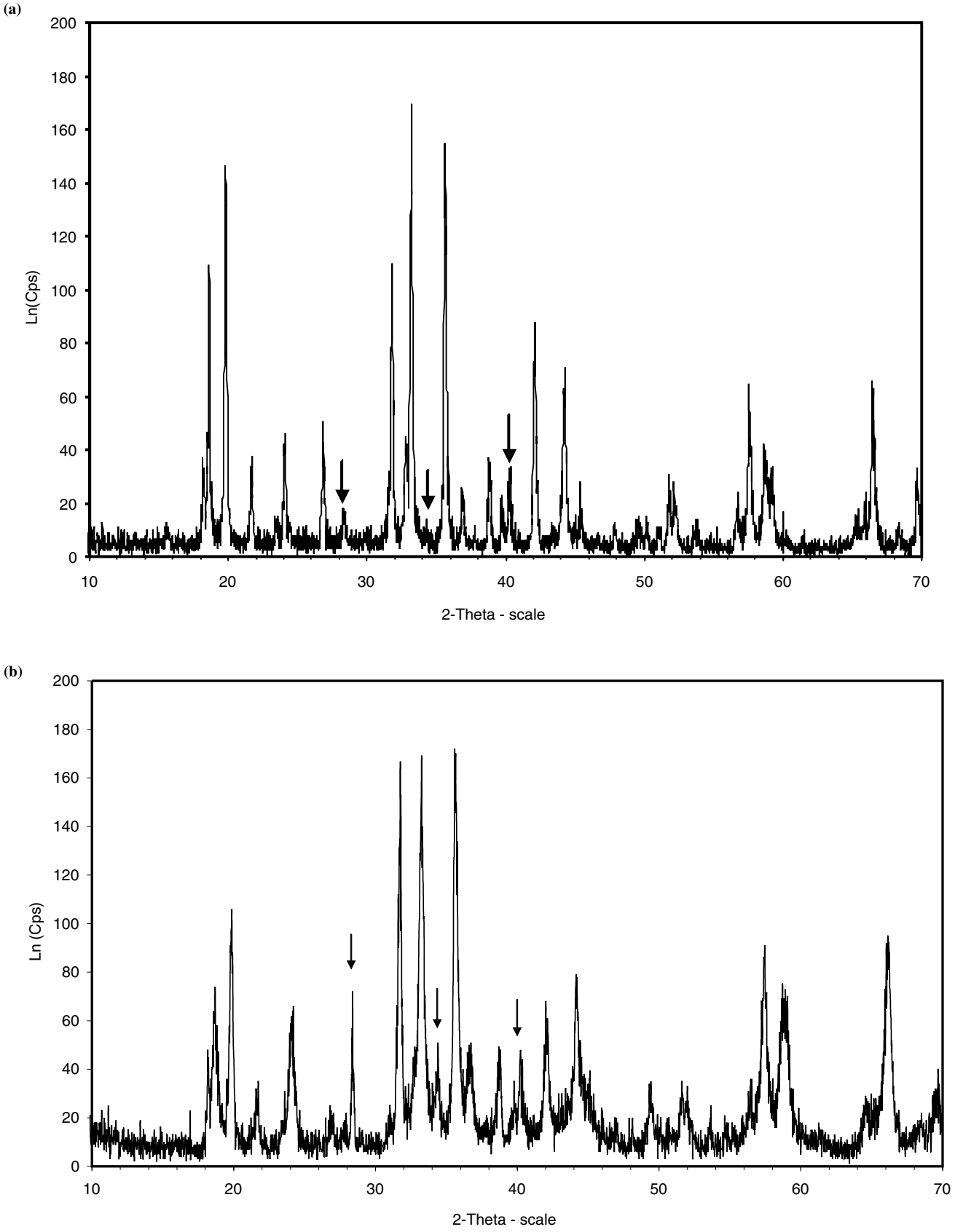

Figure 1. XRD spectra of BMA (a) and BMA–Mn (b): the lines corresponding to $BaAl_2O_4$ are pointed by arrows.

Table 1
Comparison of crystallographic parameters of different BAs

	a (Å)	c (Å)	c/a
β – alumina [11]	5.588	22.770	4.075
$BaMgAl_{10}O_{17}$ [9]	5.62	22.64	4.028
BMA[a]	5.616 ± 0.005	22.623 ± 0.037	4.028
BMA–Mn[a]	5.646 ± 0.003	22.594 ± 0.017	4.002
$BaMgAl_{10}O_{17}$ [14]	5.6224 ± 0.0001	22.6268 ± 0.0006	4.024
$BaMnAl_{10}O_{17}$ [14]	5.593 ± 0.005	22.42 ± 0.003	4.009
$BaMgAl_{10}O_{17}$[b]	5.622 ± 0.002	22.635 ± 0.013	4.026

[a]This study.
[b]Values calculated from the ICDD data with the same lines used for the samples prepared in this study.

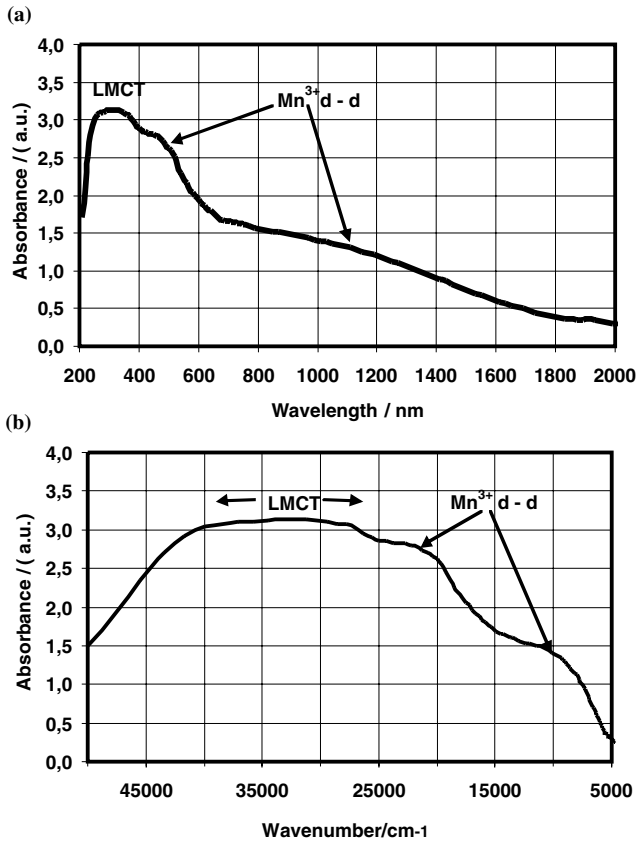

Figure 2. UV-visible diffuse reflectance spectrum for BMA–Mn. Absorbance plotted as a function of the wavelength (a) and as function of the wavenumber (b).

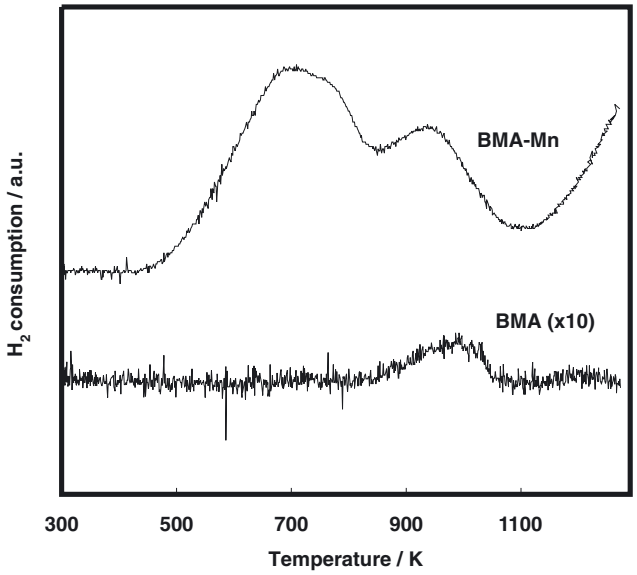

Figure 3. TPR under hydrogen of the BMA matrix and of the BMA–Mn catalyst.

4. Catalytic activity measurements

The catalytic activity was measured for the combustion of methane. A thin layer of 500 mg of catalyst was deposited over the frit of a quartz microreactor. Before the test the catalysts were activated *in situ* by treatment for 1 h at 400 °C in flowing oxygen for burning any adsorbed contaminant. After cooling down to 200 °C, the reaction is performed with a mixture of methane (1 vol%) and oxygen (4 vol%) in nitrogen, the total flow rate being 6.4 l h^{-1}. The temperature is then increased by steps of 25 K up to the temperature for which the conversion of methane is 100% (100–1100 K). Methane is totally converted in CO_2 and H_2O within the temperature range and no CO has been ever detected.

The results are shown in figure 4. For comparison, the conversions obtained previously in our laboratory for a $BaAl_{12}O_{19}$ (11 m^2 g^{-1}) matrix and a $BaMnAl_{11}O_{19}$ (14 m^2 g^{-1}) catalyst are also reported [18]. Whereas the activity of the $BaAl_{12}O_{19}$ matrix is almost nil as it should be for a support, the activity of the new host matrix $BaMgAl_{10}O_{17}$ (BMA) is very high and of the same order of magnitude as the activity of BA the $BaMnAl_{11}O_{19}$ catalyst. As well as in the case of the introduction of manganese ions increases the activity. The temperatures corresponding to 10%, 50% and 90% conversion of methane and the apparent activation energies are given in table 2 and compared to the results for the $BaMnAl_{11}O_{19}$ catalyst derived from the data of ref [18]. The activation energies are obtained by fitting the experimental data, using the least squares method, with the equation giving the conversion assuming an ideal

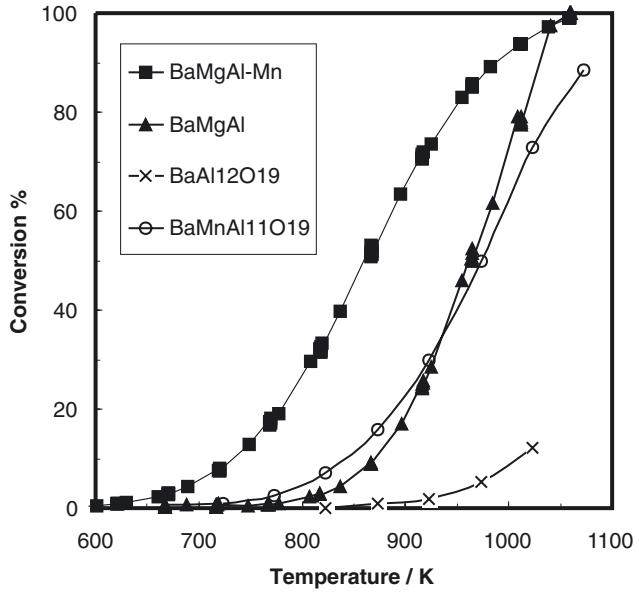

Figure 4. Catalytic conversion of methane for BMA and BMA–Mn materials, compared to the conversions for pure and Mn-doped Ba β-alumina.

Table 2
Catalytic combustion of methane on BAs

Sample	T_{10}/K	T_{50}/K	T_{90}/K	E_a/kJ mol^{-1}
BMA	870	965	1030	157
BMA–Mn	735	860	990	86
$BaMnAl_{11}O_{19}$[a]	850	975	1080	97

Values of temperatures corresponding to 10%, 50% and 90% conversions, along with apparent activation energies
[a]Values issued from reference [18].

plug flow reactor [23]. A good fit is observed for conversions up to 30%.

5. Discussion

One of the main fact is the new completely unexpected high activity of the BMA solid: the latter may even pose a problem for the nature of the true active site for transition metal substituted barium hexaluminates. So this discussion will be divided in two parts: the fist one dealing with the catalytic activity of the BMA host matrix and the second one with the effect of the introduction of the Mn ions.

When using bulk or supported metal oxides, the catalytic activity in the combustion of methane is usually attributed to the presence of a reducible cation, the reduction being experimentally confirmed by TPR measurements. Mg^{2+} is not at all a reducible cation as it is well known from Ellingham diagram (oxides reduction by hydrogen or carbon monoxide) which is confirmed by the TPR measurements shown in figure 3. The minute hydrogen consumption may be due to another reason, for example reduction of impurities present in salts used as precursors, like iron. TPR of iron(III) containing hexaaluminate starts at 773 K (partial reduction into Fe^{2+}) and ends close to 1173 K [5]. Calculation based upon integration revealed that peak intensity is lower by two orders of magnitude at least and so may well be attributed to impurities. On the other hand It is well agreed that in BMA, Mg^{2+} ions replace the Al^{3+} ions located in the spinel blocks in tetrahedral sites so-called *Al(2)* and *Al(3)* [4,11] (see figure 5a and b for clarity). The replacement of such ion cannot in any case account for the catalytic activity on this simple basis only. However it must be noted that the mirror plane is highly defective as revealed by the possibility of ion exchange [24] and high ionic conductivity [16]. The true nature of these defects has been discussed by Iyi *et al.* for Ba β-alumina [12] as well as for Mg doped K β-alumina [25]. According to the authors they consist of a Ba^{2+} vacancy associated with two Al^{3+} ions shifted from their normal position *Al(1)* to an interstitial octahedral *Al(5)* position. The introduction of Mg^{2+} instead of Al^{3+} into the tetrahedral *Al(2)* sites results in a decrease of the number of Ba^{2+} in the mirror plane and therefore in a relative increase of O^{2-} ions which can therefore account for the catalytic activity at high temperature. It must be noted that the apparent activation energy calculated for BMA of 157 kJ mol^{-1}, is quite high with respect to the energies of 97 and 86 kJ mol^{-1} calculated for the $BaMnAl_{11}O_{19}$ [18] and for the BMA–Mn catalysts respectively. This high apparent activation energy is consistent with the energy which would be expected for a mechanism controlled by the diffusion of O^{2-} ions in the mirror plane [16,26,27].

On a similar basis : Ba^{2+} vacancy associated with two Al^{3+} ions called Riedinger defects, Bellotto *et al.* [3] discussed the activity of Mn substituted Ba β-alumina. They concluded that up to a Mn/Ba $=1$ ratio most of the Mn ions are located into the *Al(2)* tetrahedral sites and that an increase of the amount of Mn giving Mn^{3+} ions located in octahedral sites do not affect significantly the catalytic activity. Theses results are in contradiction with those of Artizzu-Duart *et al.* [5,6] showing an increase of the activity with the amount of Mn^{3+} ions. This will be discussed in the following part.

As a strong analogy is evidenced between Mn and Mg doped Ba β-alumina, as far as catalytic activity is concerned, one might assume that in the BMA matrix Mg is located preferably in the tetrahedral sites, the additional Mn ions can be present as well as Mn^{2+} and Mn^{3+} ions. This introduction in the structure is clearly evidenced by the XRD analysis (figure 1 and table 1) where the 'c/a' ratio is lowered from 4.028 for BMA to 4.002 for BMA–Mn, this effect being similar to the effect of the substitution of Al by Mn in Ba β-alumina (table 1). The TPR measurements show that 28% of Mn is present as a reducible ion, and the UV-visible

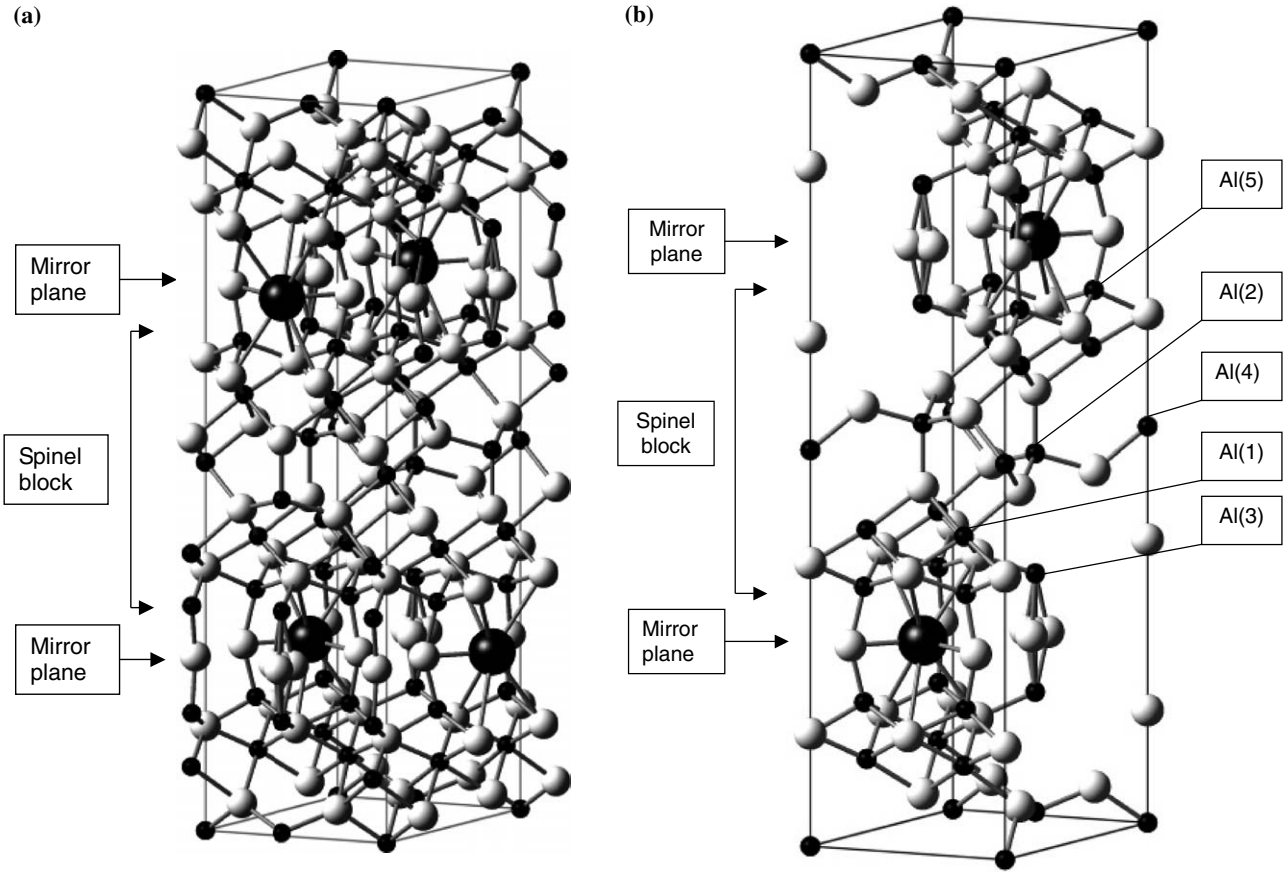

Figure 5. Location of the Al sites in a Ba β-alumina structure drawn from the positions given in 11 Al^{3+} Ba^{2+} O^{2-}. (a) General overview of the unit cell and of its environment. (b) View restricted to the internal part of the unit cell.

diffuse reflectance spectrum also reveals without any ambiguity, that some Mn^{3+} ions are present showing nevertheless some specific features. As pointed out previously the crystal structure of Mg doped Ba β-alumina has been refined by Iyi *et al.* [12] and is shown to be a typical Ba β-alumina, Mg being situated at the *Al(2)* or *Al(3)* tetrahedral sites in the spinel block. Mn^{2+} ions, which are unluckily invisible by both diffuse reflectance spectroscopy and by TPR, can be located in tetrahedral sites as well as in octahedral sites whereas Mn^{3+} is very unlikely in tetrahedral sites and prefers strongly octahedral symmetry. From the bond lengths and bond angles reported by Iyi *et al.* [12] two different octahedral sites are found in Mg doped Ba β-alumina, the *Al(1)* site which is strongly distorted, and the *Al(4)* which is more regular with equal M–O length and angles close to 90°. Moreover an extra *Al(5)* interstitial site has been also reported [4,8]. These observations agree well with the results of spectroscopic study, the distortion accounting for the forbidden transitions, whereas the possibility of location of Mn^{3+} in different sites can contribute to the widening of the metal to ligand charge transfer band: two close LMCTs may well be observed.

One might also expect that Mn^{3+} ions located in an *Al(5)* interstitial site near the mirror plane are quite easily reduced by hydrogen diffusing quickly between the spinel blocks, whereas the Mn^{3+} ions located inside a spinel block are more shielded towards reduction. This is in agreement with the observation of two reduction peaks in the TPR measurements.

In conclusion the catalytic activity or the BMA host matrix which do not show any reducible species should be attributed to the charge compensation effect due to Mg^{2+} and is probably limited by the diffusion of oxygen vacancies in the mirror plane. The extra energy necessary for diffusion (which is also an activated process) is responsible for the high activation energy in methane combustion, 50% higher than compared to usual values. When Mn is introduced in the structure, it is present mainly as Mn^{2+} ions (72%) which can contribute also to the catalytic activity by the same charge compensation mechanism as for Mg. The Mn^{3+} ions which have been evidenced by TPR and UV-visible diffuse reflectance spectra have their own catalytic activity. This is easily observed in figure 4: when comparing low conversions close to 800 K BMA containing Mn is roughly 10 times more active than the support itself. This activity

ratio is accounted for by the 28% of Mn^{3+} ions. If one could find a means to maintain all the manganese ions into the (+3) state one should obtain a attractive solid for catalytic combustion. The role of these ions is to enhance the activity through a classical Mars and van Krevelen reduction-oxidation mechanism also accounting for the lowering of the apparent activation energy.

Barium magnesium aluminium oxide BMA widely used in other fields of physics may well play a very promising role as host matrix for the preparation of high temperature combustion catalysts.

References

[1] R.A. Dalla Betta, Catal. Today 35 (1–2) (1997) 129.
[2] M. Machida, K. Eguchi and H. Arai, J. Catal. 120 (1989) 377.
[3] G. Groppi, M. Bellotto, C. Christiani, P. Forzatti and P.L. Villa, Appl. Catal. A: Gen. 104 (1993) 101.
[4] M. Bellotto, G. Artioli, C. Christiani, P. Forzatti and G. Groppi, J. Catal. 179 (1998) 597.
[5] P. Artizzu-Duart, Y. Brullé, F. Gaillard, E. Garbowski, N. Guillhaume and M. Primet, Catal. Today 54 (1999) 181.
[6] P. Artizzu-Duart, J.-M. Millet, N. Guillhaume, E. Garbowski and M. Primet, Catal. Today 59 (2000) 163.
[7] M. Machida, K. Eguchi and H. Arai, J. Catal. 103 (2000) 385.
[8] G. Groppi, F. Assandri, M. Bellotto, C. Christiani and P. Forzatti, J. Solid State Chem. 114 (1995) 236.
[9] ICDD file 26–163.
[10] ICDD file 26–135.
[11] Z. Inoue, M. Machida, K. Eguchi and H. Arai, J. Mater. Chem. 6 (1996) 455.
[12] N. Iyi, Z. Inoue, S. Takekawa and S. Kimura, J. Solid State Chem. 52 (1984) 66.
[13] J.M.P.J. Verstegen, J. Electrochem. Soc. 121 (1974) 1623.
[14] A.L.N. Stevels and A.D.M. Schrama-de Pauw, J. Electrochem. Soc. 123 (1976) 691.
[15] B.M.J. Smets and J.G. Verlijsdonk, Mater. Res. Bull. 21 (1986) 1305.
[16] T. Mathews, R. Subasri and O.M. Sreedharan, Solid State Ionics 148 (2002) 135.
[17] ICDD file 17-306.
[18] P. Artizzu Ph.D., No. 261-96, Université Claude Bernard Lyon 1, 1996.
[19] *Handbook of Chemistry and Physics*, 66th ed. (CRC Press. Boca Raton Florida, 1985–1986) p. B–113.
[20] E.R. Stobbe, B.A de Boer and J.W. Geus, Catal. Today 47 (1999) 161.
[21] A.B.P. Lever, *Inorganic Electronic Spectroscopy*, (Elsevier Publishing Company, Amsterdam, 1968) pp. 292–297.
[22] C.K. Jørgensen, *Absorption Spectra and Chemical Bonding in Complexes* (*Pergamon* Press, Oxford, 1964) p. 285.
[23] J. Villermaux, *Génie de la réaction chimique conception et fonctionnement des réacteurs*, (in French), (Lavoisier Tech et Doc, Paris, 1982) p. 238.
[24] N. Iyi, S. Takekawa and S. Kimura, J. Solid State Chem. 59 (1985) 250.
[25] N. Iyi, Z. Inoue and S. Kimura, J. Solid State Chem. 61 (1986) 236.
[26] G. He, T. Goto, T. Narushima and Y. Iguchi, Solid State Ionics 124 (1999) 119.
[27] S. Yamaguchi, Y. Iguchi and A. Amai, Solid State Ionics 40–41 (1990) 87.